Clinical Cancer Research

# Cisplatin Facilitates Radiation-Induced Abscopal Effects in Conjunction with PD-1 Checkpoint Blockade Through CXCR3/CXCL10-Mediated T-cell Recruitment

Ren Luo[1,2], Elke Firat[1], Simone Gaedicke[1], Elena Guffart[1,2], Tsubasa Watanabe[1,3], and Gabriele Niedermann[1,4,5]

## Abstract

**Purpose:** Localized radiotherapy can cause T-cell–mediated abscopal effects on nonirradiated metastases, particularly in combination with immune checkpoint blockade (ICB). However, results of prospective clinical trials have not met the expectations. We therefore investigated whether additional chemotherapy can enhance radiotherapy-induced abscopal effects in conjunction with ICB.

**Experimental Design:** In three different two-tumor mouse models, triple therapy with radiotherapy, anti–PD-1, and cisplatin (one of the most widely used antineoplastic agents) was compared with double or single therapies.

**Results:** In these mouse models, the response of the nonirradiated tumor and the survival of the mice were much better upon triple therapy than upon radiotherapy + anti–PD-1 or cisplatin + anti–PD-1 or the monotherapies; complete regression of the nonirradiated tumor was usually only observed in triple-treated mice. Mechanistically, the enhanced abscopal effect required $CD8^+$ T cells and relied on the CXCR3/CXCL10 axis. Moreover, CXCL10 was found to be directly induced by cisplatin in the tumor cells. Furthermore, cisplatin-induced $CD8^+$ T cells and direct cytoreductive effects of cisplatin also seem to contribute to the enhanced systemic effect. Finally, the results show that the abscopal effect is not precluded by the observed transient radiotherapy-induced lymphopenia.

**Conclusions:** This is the first report showing that chemotherapy can enhance radiotherapy-induced abscopal effects in conjunction with ICB. This even applies to cisplatin, which is not classically immunogenic. Whereas previous studies have focused on how to effectively induce tumor-specific T cells, this study highlights that successful attraction of the induced T cells to nonirradiated tumors is also crucial for potent abscopal effects.

## Introduction

Immune checkpoint blockade (ICB) has revolutionized cancer therapy. Strong durable responses, however, are limited to a proportion of patients with immunogenic tumors. Improvements are therefore urgently needed (1). One possible way to enhance the immunogenicity of tumors and to improve ICB responses is by combination with radiotherapy (2, 3). Contrary to previous assumptions, research has shown that localized radiotherapy can promote tumor-specific $CD8^+$ T-cell responses (4). These T-cell responses contribute to the control of the irradiated tumor and can also trigger systemic (so-called abscopal) effects on nonirradiated metastases, especially in conjunction with ICB (2, 3). Abscopal effects can be readily induced in optimized tumor models in mice and have been described in case reports and retrospective clinical trials (5). The first prospective RT/ICB trials in metastatic patients have also provided evidence for systemic effects of local radiotherapy (6–11), but the results did not meet the expectations (12, 13). Stronger abscopal effects may be achieved by adjustments in the administration of combined radiotherapy/ICB or by the addition of other therapeutics.

Certain anticancer chemotherapeutic agents are also immunogenic and elicit immune-mediated antitumor effects (14). Recent trials have shown that the combination of chemotherapy with ICB can significantly improve the response rates compared with the respective monotherapies (15, 16). However, complete responses are still very rare; therefore, improvements are needed here as well.

It is controversial whether cisplatin is immunogenic (14, 17–22). Cisplatin is one of the most widely used chemotherapeutic agents for the treatment of solid tumors (23) and is actually the most commonly used chemotherapeutic agent in radiation oncology (24). Recently, Kroon and colleagues (25), using a two-tumor breast cancer model, reported that the quadruple combination of radiotherapy + anti–PD-1 + anti-CD137 + cisplatin was more effective against the nonirradiated tumor

[1]Department of Radiation Oncology, Faculty of Medicine, University of Freiburg, Freiburg, Germany. [2]Faculty of Biology, University of Freiburg, Freiburg, Germany. [3]Institute for Integrated Radiation and Nuclear Science, Kyoto University, Osaka, Japan. [4]German Cancer Consortium (DKTK), Partner Site Freiburg, Freiburg, Germany. [5]German Cancer Research Center (DKFZ), Heidelberg, Germany.

**Note:** Supplementary data for this article are available at Clinical Cancer Research Online (http://clincancerres.aacrjournals.org/).

**Corresponding Author:** Gabriele Niedermann, Department of Radiation Oncology, Faculty of Medicine, University of Freiburg, Robert-Koch-Strasse 3, Freiburg 79106, Germany. Phone: 4976-1270-95140; Fax: 4976-1270-95130; E-mail: gabriele.niedermann@uniklinik-freiburg.de

Clin Cancer Res 2019;25:7243–55

**doi:** 10.1158/1078-0432.CCR-19-1344

## Translational Relevance

Systemic (abscopal) effects of local radiotherapy in conjunction with immune checkpoint blockade are only rarely observed in patients and may be limited by inadequate infiltration of radiotherapy-induced tumor-specific T cells into the nonirradiated metastases. Cisplatin is one of the most widely used antineoplastic agents. We show in mice that cisplatin can dramatically enhance radiotherapy-induced abscopal effects in conjunction with anti–PD-1. This was crucially dependent on the recruitment of T cells expressing the chemokine receptor CXCR3 and the chemokine CXCL10, which is directly induced by cisplatin in the tumor cells. In addition, the data indicate that cisplatin-induced $CD8^+$ T cells and direct cytoreductive effects of cisplatin also contribute to the enhanced abscopal effect. Although cisplatin is not regarded as classically immunogenic, our data suggest that adding it to radiotherapy + anti–PD-1 may increase abscopal effects in patients, particularly through the induction of the T-cell–attracting chemokine CXCL10 in the nonirradiated metastases.

than the triple combination of radiotherapy + anti–PD-1 + anti-CD137. However, the quadruple combination was not better than the triple combination of cisplatin + anti–PD-1 + anti-CD137. Thus, the better response of the nonirradiated tumor did not reflect an enhanced radiotherapy-induced abscopal effect but merely reflected an effect of cisplatin on the nonirradiated tumor. Moreover, it remained unclear whether the effect of cisplatin on the nonirradiated tumor depended on the immune system.

Here, we show, in three syngeneic tumor models, that the addition of cisplatin to radiotherapy + anti–PD-1 can facilitate radiotherapy-induced abscopal effects in conjunction with ICB and provoke much better systemic responses than either radiotherapy + anti–PD-1 or cisplatin + anti–PD-1. We also revealed mechanisms by which cisplatin enhances radiotherapy-induced T cell–mediated abscopal effects.

## Materials and Methods

### Mice and cell lines

All animal experiments were performed in accordance with the German Animal License Regulations and were approved by the animal care committee of the Regierungspräsidium Freiburg (registration numbers: G19-062). C57BL/6Nrj mice and BALB/c mice were purchased from Janvier Labs and kept under standard pathogen-free conditions. To generate CD133-expressing melanoma cells (B16-CD133), B16-F10 cells were transduced with lentiviral particles encoding the human stem cell marker CD133 and cultured as described previously (26). MC38 murine adenocarcinoma cells were purchased from Kerafast. C51 colon carcinoma cells were kindly provided by Mario Paolo Colombo (Fondazione IRCCS Istituto Nazionale dei Tumori, Milan, Italy).

### Tumor models and treatment

B16-CD133, MC38, or C51 tumor cell suspensions were mixed with Matrigel (Corning) and injected subcutaneously into the right flank (primary tumor) and left flank (secondary tumor) of 6- to 8-week-old C57BL/6Nrj or BALB/c mice, respectively. The final Matrigel concentration was 50%. For the B16-CD133 model, the mice were implanted with $2 \times 10^5$ cells in the right flank, and 5 days later, in the left flank. In the MC38 model, $5 \times 10^5$ cells were injected into the right flank, and 4 days later, $3 \times 10^5$ cells were injected into the left flank. In the C51 model, $5 \times 10^5$ cells were injected into the right flank, and 6 days later, $5 \times 10^5$ cells were injected into the left flank. The tumor sizes were measured with calipers, and the volumes were calculated using the formula: length $\times$ width $\times$ height.

Mice with a predefined size range for both the primary and secondary tumor were assigned randomly to the experimental groups. In the B16-CD133 model, two consecutive fractions of local hypofractionated radiotherapy (hRT) of 12 Gy each were delivered when the primary and secondary tumors reached a volume of 450 to 525 $mm^3$ and 125 to 175 $mm^3$, respectively (approximately day 11 after primary tumor inoculation). In the MC38 model, three fractions of local hRT of 8 Gy each on consecutive days were delivered when the primary and secondary tumors reached a volume of 250 to 350 $mm^3$ and 130 to 150 $mm^3$, respectively (approximately day 10 after primary tumor inoculation). In the C51 model, two fractions of local hRT of 8 Gy each on consecutive days were delivered when the primary and secondary tumors reached a volume of 400 to 600 $mm^3$ and 100 to 180 $mm^3$, respectively (approximately day 12 after primary tumor inoculation). hRT dose and fractionation for the different tumor models were chosen according to references (27–29). Tumor irradiation was performed using an RS2000 X-ray unit (RadSource). Anesthetized mice were positioned in a custom-made plastic jig with a size-adjustable aperture for the primary tumor; the rest of the mouse body was fully shielded with lead. Weekly intraperitoneal injections of anti–PD-1 antibody (200 μg; clone RMP1-14, Bio X Cell) or isotype control antibody (200 μg; clone 2A3, Bio X Cell) were started at the first day of radiotherapy. Cisplatin (ab141398, Abcam) was injected at 5 mg/kg intraperitoneally into mice once on day 0 of therapy. In some experiments, $CD8^+$ T cells were depleted by injecting 200 μg/mouse of anti-CD8 antibodies (clone 2.43, Bio X Cell) intraperitoneally 3 days before hRT, on the day of the first hRT, and once weekly thereafter. In the CXCR3 blockade experiment, 50 μg/mouse of anti-CXCR3 antibody (clone CXCR3-173, Bio X Cell) was injected intraperitoneally 2 days before hRT, on the first day of hRT, and maintained every 3 days in a total of five doses. Survival was defined as the time point after the start of treatment when either the primary or the secondary tumor had reached a size of 2,000 $mm^3$.

The mice were ear-tagged and not grouped together according to treatment group. Therefore, in tumor follow-up and analysis of tissue samples, the experimenter was not aware of the treatment the individual mice had received. However, because the same experimenter performed all experiments and analyses, the experiments were not conducted in a completely blinded fashion.

### Hematologic assessment

Blood samples were obtained from the tails of mice and were collected in EDTA·K2 tubes (Microvette CB 300 K2E). Complete blood cell counts were performed by the URIT-5250 hematology analyzer (URIT Medical Electronic Co. Ltd.).

### Preparation of single-cell suspensions from tumors, lymphatic organs, and blood

Primary and secondary tumors were weighed and digested in 10 mL of PBS plus $MgCl_2$ plus $CaCl_2$ (Gibco; Thermo Fisher

Scientific) supplemented with 1,000 U DNase I (New England BioLabs), 10 mmol/L $MgCl_2$ (Sigma-Aldrich), and 0.7 U/mL Liberase-Blendzyme solution (Roche Life Science) for 30 minutes at 37°C. Single-cell suspensions were filtered through a 30-μm preseparation filter (Miltenyi Biotec). The spleens and lymph nodes were squeezed through a 70-μm strainer. Red blood cell lysis was performed using 1× red blood cell lysis buffer (eBioscience).

### Flow cytometric analyses

Flow cytometric analyses of tumor-infiltrating lymphocytes and single-cell suspensions from spleen, blood, and lymph nodes were performed using the following antibodies/MHC tetramer. M8 tetramer-PE (H-2K$^b$, p15E) and AH1 tetramer-PE (H-2L$^d$, gp70; both from Baylor College of Medicine, Houston, TX) with CD8-FITC (clone KT15, MBL) were used to detect tumor-specific CD8$^+$ T cells. CXCR3-APC (clone CXCR3-173) and CD133/1-PE (clone AC133) were from Miltenyi Biotec. CD3-BV421 (clone 390), CD3-PerCP-Cy5.5 (clone 145-2C11), CD8-AF700 (clone 53-6.7), CD4-BV510 (clone RM4-5), Ki-67-BV605 (clone 16A8), CD45-BV510 (clone 30-F11), CD11b-PE-Cy7 (clone M1/70), Ly6C-BV605 (clone HK1.4), CD127-BV421 (clone A7R34), CD62L-APC-Cy7 (clone MEL-14), and CD103-BV421 (clone 2E7) were purchased from BioLegend. Other antibodies used were: CD31-BV421 (clone 390, BD Bioscience), NK1.1-PE-Cy7 (clone PK136), MHCII-PE (clone M5/114.15.2), CD44-FITC (clone IM7), and CD11c-APC (clone N418, all from eBioscience).

For intracellular staining of CXCL10, brefeldin A (eBioscience) was added to tumor single-cell suspensions (final concentration, 3.0 μg/mL) and incubated in a $CO_2$ incubator at 37°C for 6 hours. After surface marker staining, the cells were fixed and permeabilized using buffers and protocols from eBioscience (00-8222-49/56). CXCL10 (AF-466-NA) antibody and its goat IgG isotype control (AB-108-C) were from R&D Systems and used as primary antibodies. The secondary antibody (rabbit anti-goat IgG (H+L), Alexa Fluor 488) was from Thermo Fisher Scientific.

7-AAD (BD Bioscience) or Zombie Red (BioLegend) was used to exclude dead cells. The samples were analyzed using a FACSVerse (BD Biosciences) flow cytometer or a CytoFLEX S flow cytometer (Beckman Coulter). Data analysis was performed using FlowJo software (version 10.4.0). Dendritic cell (DC) populations were identified with a previously described marker combination (30): (Ly6C$^+$) CD103$^+$ DCs: CD45$^+$, MHCII$^+$, CD11c$^+$, CD11b$^{dim}$, CD103/CD8a$^+$, (Ly6C$^+$); conventional DCs (cDC): CD45$^+$, MHCII$^+$, CD11c$^+$, CD11b$^{dim}$, CD103/CD8a$^-$; monocyte-derived DCs (moDC): CD45$^+$, MHCII$^+$, CD11c$^+$, CD11b$^{high}$; macrophages (MF): CD45$^+$, MHCII$^+$, CD11c$^-$, CD11b$^+$.

### ELISA

For *in vitro* experiments, before adding cisplatin or IFNγ to the cells, the culture medium was refreshed. After treatment (48 hours with cisplatin; 24 hours with IFNγ), supernatant was collected and measured. Measured concentrations were normalized on the basis of the number of viable cells. In *ex vivo* experiments, proteins from nonirradiated secondary tumors were isolated using RIPA lysis buffer supplemented with protease inhibitor cocktail (Roche) and the phosphatase inhibitors NaF and $Na_3VO_4$ (Sigma). Pierce BCA Protein Assay Kit was used to measure the concentration of whole protein in tumor lysates before ELISA measurement. Mouse IP-10 (CXCL10) Module Set ELISA (BMS6018MST, eBioscience) was used for the detection of CXCL10 in tumor lysates according to the manufacturer's protocol.

### Western blot analysis

Brefeldin A (eBioscience) was added to treated B16-CD133 cells (final concentration, 3.0 μg/mL) at 37°C for 4 hours. Cells were lysed in RIPA lysis buffer supplemented with protease inhibitor cocktail (Roche) and the phosphatase inhibitors NaF and $Na_3VO_4$ (Sigma). Cell lysate (30 μg) was separated by SDS-PAGE and blotted onto nitrocellulose. The blots were developed for CXCL10 (LS-C104402, LifeSpan BioSciences). HRP-conjugated secondary antibodies were purchased from Dianova. The amount of loaded protein was normalized to GAPDH mAb (ab9485, Abcam).

### *In vitro* cytotoxicity of cisplatin

B16-CD133 cells were plated at $1 \times 10^5$ cells in 12-cm plates and allowed to adhere overnight prior to treatment with cisplatin (1, 2.5, or 5 mg/L, 48-hour incubation). The FITC Annexin V/PI Kit (Miltenyi Biotec) was used to determine the proportion of apoptotic cells. Intranuclear staining for Ki-67 was performed using the Transcription Factor Staining Buffer Set (eBioscience). Cell viability and the $IC_{50}$ were assessed by the 3-(4,5-dimethylthiazol-2-yl)-2,5-diphenyltetrazoliumbromide (MTT) assay. Briefly, 5,000 B16-CD133 cells were seeded per well in 96-well plates. After 48 hours of incubation, 20 μL of MTT (5 mg/L) in Dulbecco's PBS was added to each well and cells were further incubated for 4 hours. Medium was removed and MTT formazan crystals were solubilized by 100 μL of DMSO per well. Absorbance of each well was measured with a microplate reader at 550 nm. Untreated wells were used as controls.

### Analysis of cell surface expression of calreticulin

Cells were plated at $1 \times 10^6$ cells in 12-cm plates and allowed to adhere overnight prior to treatment. B16-CD133 cells were exposed to cisplatin (1 or 5 mg/L) for 48 hours; thereafter, cisplatin was removed by exchanging the medium. In irradiation experiments, the cells were exposed to two fractions of 12 Gy each on consecutive days using a Gammacell 40 $^{137}$Cs laboratory irradiator. On days 2, 4, and 6 after the second irradiation or after the removal of cisplatin, cells were trypsinized and stained with calreticulin-Alexa Fluor 488 (EPR3924, Abcam) antibody or isotype control antibody (Alexa Fluor 488, EPR25A, Abcam). 7-AAD (BD Biosciences) was used to exclude the dead cells.

### Statistical analysis

Previous experience served as the basis for calculations of expected averages and deviations used to calculate sample size to detect an effect with power = 0.8. This typically resulted in a minimum sample size of $n = 5$–7, depending on the experiment. For two-group comparison, statistical analysis was performed using an unpaired two-tailed Student *t* test. For multiple comparisons, one-way ANOVA followed by the "Two-stage step-up method of Benjamini, Krieger and Yekutieli" was used. Survival data were compared using the log-rank Mantel–Cox test. $P < 0.05$ ($P < 0.05$, $P < 0.01$, $P < 0.001$, $P < 0.0001$) was considered statistically significant. All analyses were performed using Prism version 7.0 (GraphPad).

## Results

### Cisplatin facilitates radiotherapy-induced abscopal effects in combination with anti–PD-1

We investigated whether cisplatin can enhance radiotherapy-induced abscopal effects in mouse models with two tumors (in opposite flanks) in which the primary was irradiated, but not the secondary tumor (Fig. 1A). First, we used an immunogenic B16 melanoma model transfected with the human stem cell antigen CD133 (26, 31). The primary tumor was treated with hRT, delivering the total radiotherapy dose in two fractions of 12 Gy on consecutive days. In addition, the mice received systemic anti–PD-1 antibody once per week. Triple-treated mice also received a single dose of cisplatin together with the first radiotherapy fraction.

Anti–PD-1 monotherapy was not effective in this aggressive model (Fig. 1B). Local hRT induced transient growth arrest of the irradiated tumor. hRT + anti–PD-1 was more effective against the primary tumor, and it induced a substantial synergistic abscopal effect ($P < 0.001$, compared with anti–PD-1 and radiotherapy monotherapies; Fig. 1B, right), but there were no cures of the nonirradiated secondary tumor. Although cisplatin alone did not affect the primary tumor, it suppressed the smaller secondary tumor ($P < 0.01$, compared with untreated mice; Fig. 1B; Supplementary Fig. S1A and S1C). Radiotherapy + cisplatin was effective against the primary but did not improve the response of the secondary tumor compared with cisplatin monotherapy. Cisplatin + anti–PD-1 had an effect similar to hRT + anti–PD-1 on the secondary tumor, and it is worth noting that it slowed the growth of the large primary tumor, although the respective monotherapies were completely ineffective. However, triple therapy with hRT + anti–PD-1 + cisplatin was best. The survival time of triple-treated mice almost doubled compared with the second-best treatment (hRT + anti–PD-1; $P < 0.0001$; Fig. 1C). Particularly striking was the much better effect on the nonirradiated secondary tumor ($P < 0.01$, compared with radiotherapy + anti–PD-1 or cisplatin + anti–PD-1; Fig. 1B, right; Supplementary Fig. S2A). From about day 10 after start of the triple therapy, regression of the nonirradiated secondary tumor was observed (Fig. 1B and D, right). Although no secondary tumor was eradicated upon hRT + anti–PD-1, 50% of the triple-treated mice showed complete regression (CR) of the nonirradiated secondary tumor (Fig. 1D, right).

Similar results were obtained in the MC38 colon carcinoma model (Fig. 1E). Also, in this model, triple treatment was better than hRT + anti–PD-1 (Fig. 1E and F; Supplementary Fig. S2B), although the survival advantage was not as strong as in the B16-CD133 model (Fig. 1F). In the MC38 model, triple treatment was much better than cisplatin + anti–PD-1, both in terms of response of the primary and secondary tumors and overall survival (Fig. 1E and F). As in the B16-CD133 model, cisplatin monotherapy did not significantly affect the primary tumor (Fig. 1E; Supplementary Fig. S1B). Whether cisplatin reduced the growth of the smaller secondary tumor was difficult to judge as the mice had to be sacrificed very early because of the rapidly growing primary tumor (Fig. 1E and F). However, an experiment in mice carrying a single tumor demonstrated that cisplatin did reduce the growth of MC38 tumors of the size of the metastasis compared with untreated mice (Supplementary Fig. S1D).

As a third model, we used the radiosensitive C51 colon carcinoma model, which also showed sensitivity to cisplatin ($P < 0.001$ and $P < 0.05$, compared with anti–PD-1 in the left and right panel of Fig. 1G, respectively). Also, in this model, triple therapy was best (Fig. 1G–I; Supplementary Fig. S2C and S2D), and even though only two fractions of 8 Gy were used, both the irradiated primary and the nonirradiated secondary tumor were cured in almost all triple-treated mice. In contrast, no mouse was cured with radiotherapy + anti–PD-1 and only one of seven mice was cured with cisplatin + anti–PD-1.

Taken together, our results showed that the addition of cisplatin to hRT + anti–PD-1 can greatly improve radiotherapy-induced abscopal effects in conjunction with anti–PD-1 and promote survival of the mice in comparison with both hRT + anti–PD-1 and cisplatin + anti–PD-1. Moreover, the effect of the triple therapy on the nonirradiated tumor appeared to be more than additive.

### The enhanced abscopal effect strongly depended on $CD8^+$ T cells and correlated with a robust tumor-specific $CD8^+$ T-cell response

To elucidate the mechanisms underlying the superior response to triple therapy, mice bearing B16-CD133 melanomas were treated with hRT + anti–PD-1 + cisplatin or with cisplatin + anti–PD-1, in addition to antibodies to deplete $CD8^+$ T cells (Fig. 2A). The two doses of the depleting antibody caused a complete longer lasting depletion of the $CD8^+$ T cells in the peripheral blood of the mice (Supplementary Fig. S3). As shown in Fig. 2B and C, the effect of both double and triple therapy on the nonirradiated tumor strongly depended on $CD8^+$ T cells. The effect on the primary tumor also clearly depended on $CD8^+$ T cells; however, in triple-treated mice, this became evident only after about 12 days, probably because of the strong direct antitumor effect of hRT (Fig. 2B, left).

In accordance with the T-cell depletion results, flow cytometry analysis of tumor single-cell suspensions showed that triple treatment induced an increase in the proportion and the density (per gram tumor) of tumor-specific $CD8^+$ T cells both on day 7 and on day 12 after start of treatment (Fig. 2D). At day 12, on average, triple treatment caused a more than 10-fold increase in the density of tumor-specific $CD8^+$ T cells in the irradiated and the nonirradiated tumor, compared with anti–PD-1 monotherapy (Fig. 2D, bottom).

The cisplatin/anti–PD-1 double combination also induced more tumor-specific $CD8^+$ T cells in the nonirradiated tumor than anti–PD-1 monotherapy, but this response could only be detected at day 12 and not yet on day 7 (Fig. 2D, bottom and top right). The ratio of tumor-specific tetramer+ $CD8^+$ T cells to tumor cells was also increased compared with anti–PD-1 monotherapy (Supplementary Fig. S4A and S4B).

Taken together, these results demonstrated that the antitumor efficacy of the triple therapy strongly depended on $CD8^+$ T cells and suggested that tumor-specific $CD8^+$ T cells induced by cisplatin + anti–PD-1 contributed to the enhanced radiotherapy-mediated abscopal effect in triple-treated mice.

### Long-lasting $CD8^+$ T-cell memory responses in cured triple-treated mice

In addition, we measured tumor-specific memory $CD8^+$ T-cell responses in triple-treated mice that had been cured from C51 tumors. A significant number of tumor antigen-specific tetramer+ $CD8^+$ T cells was detected in blood and secondary lymphoid organs 3 months after the cure (Supplementary Fig. S5A). Approximately 50% of these tetramer+ cells showed a central memory

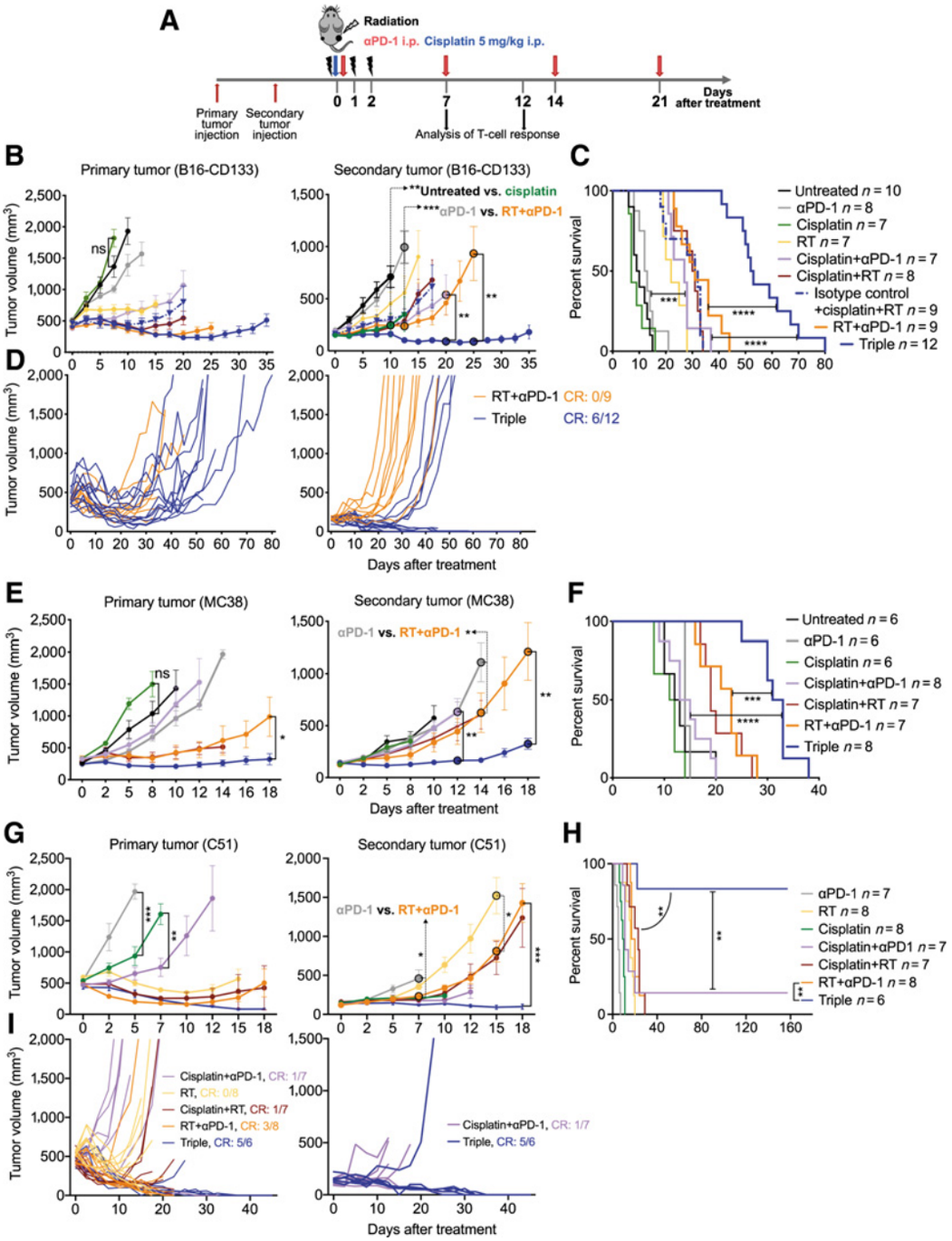


**Figure 1.**

Concurrent cisplatin facilitates radiation-induced abscopal effects in conjunction with anti–PD-1. **A,** Scheme for treatments and T-cell analyses. **B,** B16-CD133 tumor growth of primary (left) and secondary tumors (right; asterisks indicate *P* values for the comparison of certain groups using a two-tailed *t* test as indicated in the figure). **C,** Survival of mice (log-rank test; $n = 7$–12 mice/group). **D,** Individual tumor growth curves for primary and secondary B16-CD133 tumors in mice treated with RT + anti–PD-1 or triple therapy. **E,** Tumor growth of primary (left) and secondary MC38 tumors (right; asterisks indicate *P* values for the comparison of certain groups using a two-tailed *t* test as indicated in the figure). **F,** Survival of mice bearing bilateral MC38 tumors for different treatment groups (log-rank test; $n = 6$–8 mice/group). **G,** C51 tumor growth of primary (left) and secondary tumors (right; asterisks indicate *P* values for the comparison of certain groups using a two-tailed *t* test as indicated in the figure). **H,** Survival of mice bearing bilateral C51 tumors for different treatment groups (log-rank test; $n = 6$–8 mice/group). **I,** Individual tumor growth curves for primary and secondary C51 tumors. All data are presented as mean ± SEM. ns, not significant; *, $P < 0.05$; **, $P < 0.01$; ***, $P < 0.001$; ****, $P < 0.0001$.

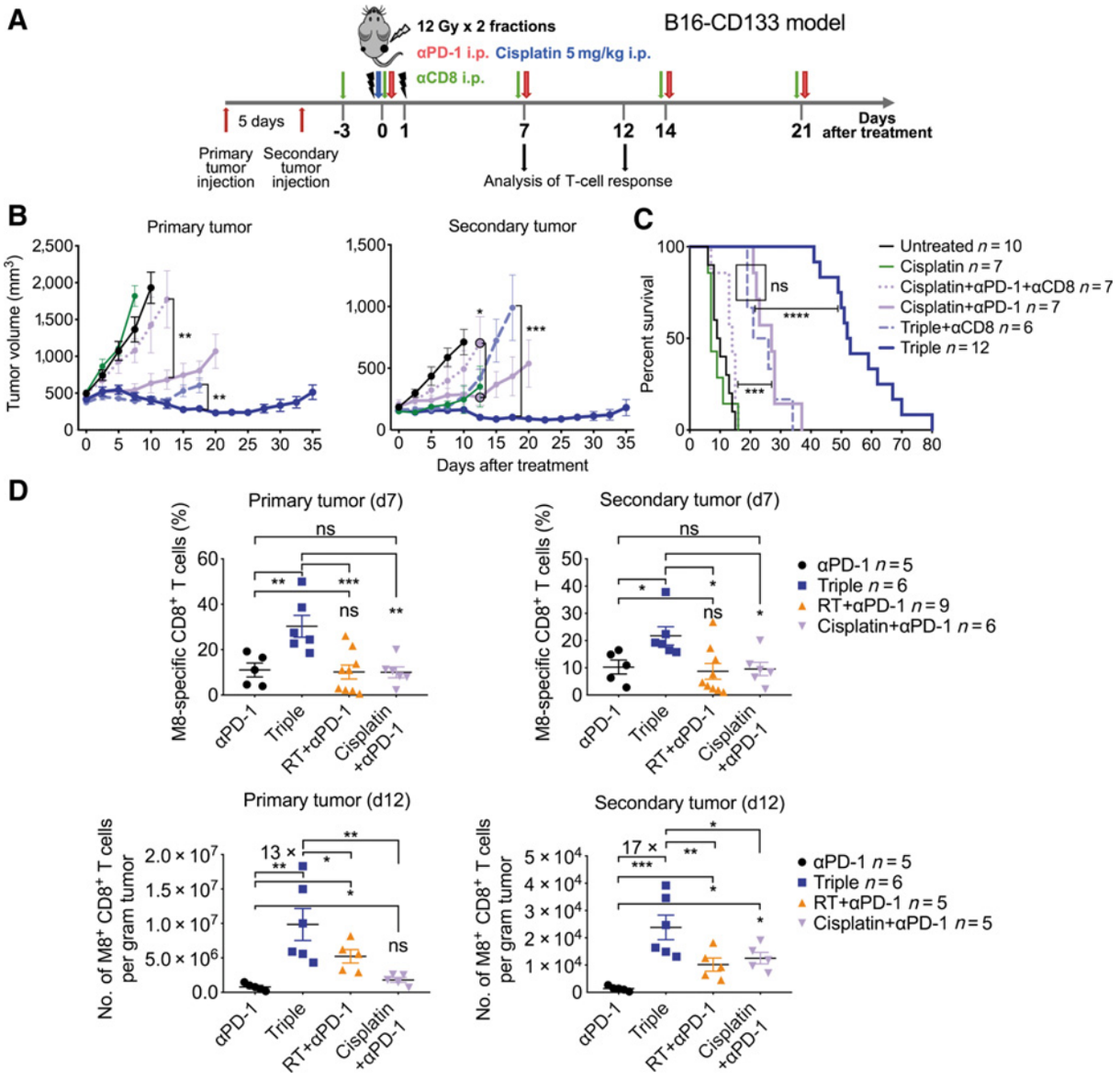


**Figure 2.**

Abscopal tumor regression upon triple therapy with RT, cisplatin, and anti–PD-1 strongly depends on CD8$^+$ T cells and correlates with tumor-specific CD8$^+$ TILs. **A,** Scheme for the depletion of CD8$^+$ T cells. **B,** B16-CD133 tumor growth of irradiated primary (left) and nonirradiated secondary tumors (right) (asterisks indicate *P* values for the comparison of certain groups using a two-tailed *t* test as indicated in the figure). **C,** Survival of mice (log-rank test; $n = 6$–12 mice/group). **D,** M8 tetramer-positive tumor-specific T cells on day 7 (top) and day 12 (bottom) in primary and secondary tumors ($n = 5$–9 mice/group). All data are presented as mean ± SEM. ns, not significant; *, $P < 0.05$; **, $P < 0.01$; ***, $P < 0.001$; ****, $P < 0.0001$.

phenotype and almost all of these T cells expressed the IL7 receptor. Effector and central memory T cells also increased in the total CD8$^+$ T-cell population compared with naïve mice (Supplementary Fig. S5B). These data showed that a single dose of 5 mg/kg cisplatin did not prevent the formation of memory CD8$^+$ T cells in triple-treated mice.

### Correlation of the abscopal effect with expression of the T-cell chemoattractant CXCL10 in the nonirradiated tumor

Tumor-specific CD8$^+$ T cells induced by cisplatin or cisplatin + anti–PD-1 may suppress the nonirradiated tumor not only through T-cell–mediated cytotoxicity. They could also recruit more CXCR3$^+$ tumor-specific T cells, including RT- and chemotherapy-induced CD8$^+$ T cells, to the nonirradiated tumor by secretion of the effector cytokine IFNγ. IFNγ is known to induce the expression of the T-cell–attracting chemokines CXCL9, CXCL10, and CXCL11 (32); see also Supplementary Fig. S6A. Of note, certain chemotherapeutic agents induce T-cell–recruiting chemokines, mainly CXCL10, directly in tumor cells (19, 33). The great advantage could be that infiltration of tumor-specific T cells could be enhanced even in cold tumors. However, whether cisplatin directly induces the

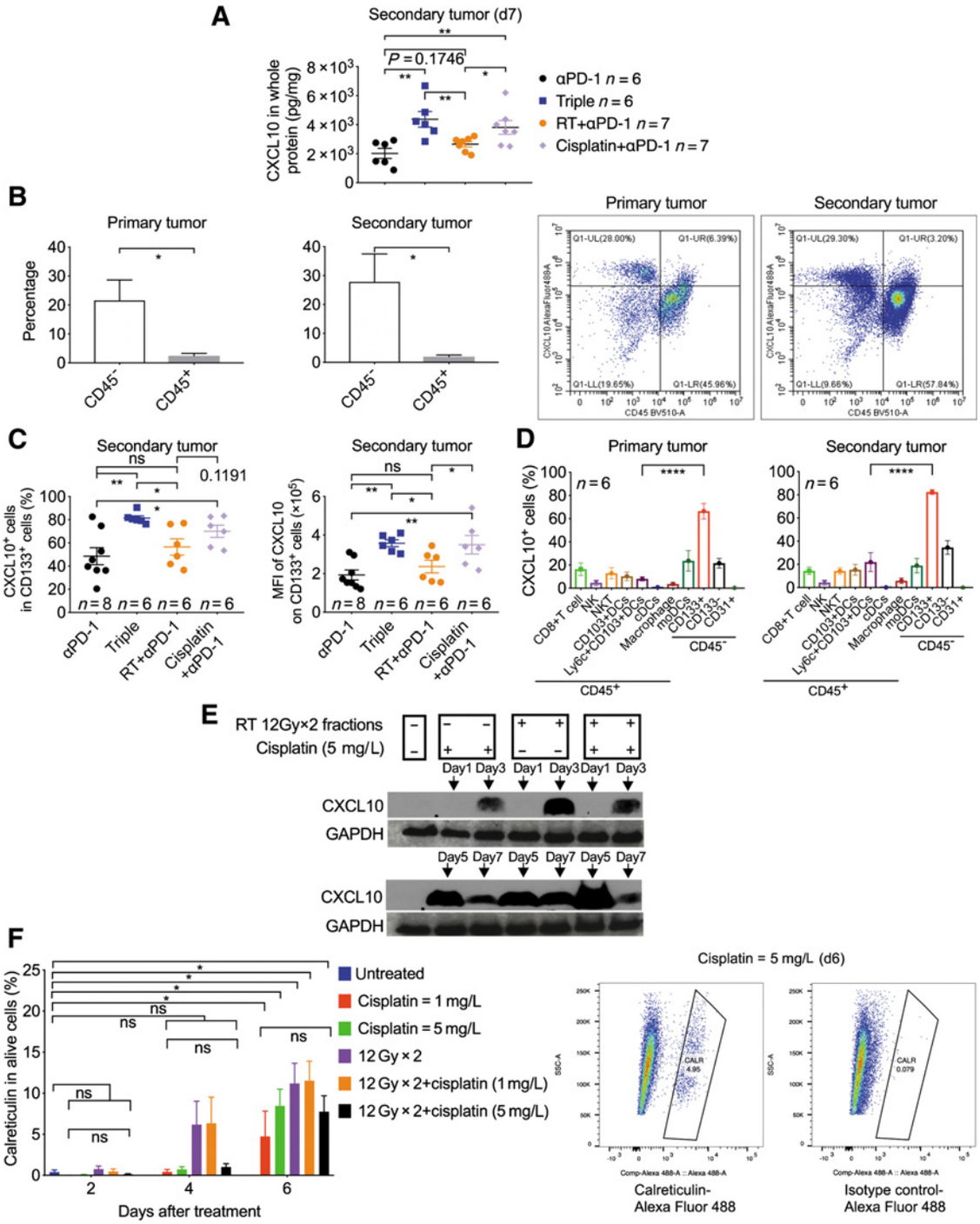


**Figure 3.**

Expression of the immunogenic mediators CXCL10 and calreticulin. **A,** CXCL10 concentration in nonirradiated B16-CD133 secondary tumors 7 days after therapy measured by ELISA. **B,** Flow cytometric determination of the proportion of CXCL10-secreting CD45$^-$ and CD45$^+$ cells in tumor single-cell suspensions. Mice ($n$ = 6) on day 7 of triple therapy. Examples of flow cytometry plots are shown on the right side. **C,** Percentage of CXCL10$^+$ CD133$^+$ tumor cells in secondary tumors 7 days after therapy and CXCL10 median fluorescence intensity (MFI) of CD133$^+$ tumor cells measured by flow cytometry ($n$ = 6–8 mice/group). **D,** Percentage of CXCL10$^+$ cells in various CD45$^+$ and various CD45$^-$ tumor cell subpopulations in primary and secondary B16-CD133 tumors. Mice ($n$ = 6) treated with triple therapy. Tumor samples were harvested and analyzed by flow cytometry 7 days after therapy. **E,** CXCL10 expression in B16-CD133 cells treated *in vitro* with cisplatin and/or radiation as determined by Western blot analysis (one of two independent experiments with similar results is shown). **F,** Percentage of calreticulin$^+$ 7-AAD$^-$ B16-CD133 cells after treatment with cisplatin and/or radiation (from three independent experiments). Examples for flow cytometric analyses on day 6 are shown on the right side. All data are presented as mean with SEM. ns, not significant; $^*$, $P < 0.05$; $^{**}$, $P < 0.01$; $^{***}$, $P < 0.001$; $^{****}$, $P < 0.0001$.

expression of CXCL10 is controversial (19, 33). We therefore examined CXCL10 expression in both irradiated and nonirradiated tumors following the different treatment regimens directly *ex vivo* as well as following the genotoxic treatments of the tumor cells *in vitro*.

As shown in Fig. 3A, both triple therapy and cisplatin + anti–PD-1 significantly increased the CXCL10 expression in the nonirradiated tumor, compared with anti–PD-1 monotherapy ($P < 0.01$), whereas this was not observed upon treatment with hRT + anti–PD-1. Both in the primary and the secondary tumor, CXCL10 was mainly expressed by nonleukocyte cell types ($CD45^-$ cells; Fig. 3B). Moreover, among the $CD45^-$ cells, a high proportion of the tumor cells, which are $CD133^+$, expressed CXCL10, particularly after triple therapy and after cisplatin + anti–PD-1 (Fig. 3C). Also, compared with the infiltrating leukocytes, including various types of DCs, tumor cell expression of CXCL10 appeared to be considerably higher (Fig. 3D).

*In vitro* experiments revealed that nontreated B16-CD133 melanoma cells express only very low levels of CXCL10 (not visible within the exposure time used in Fig. 3E). However, several days after treatment with either two fractions of 12 Gy or cisplatin (5 mg/L, $IC_{50}$), or both, CXCL10 was robustly expressed by the melanoma cells. Cisplatin-induced CXCL10 expression was higher on day 5 after the exposure than on day 3. CXCL10 was also secreted by MC38 cells upon exposure to cisplatin *in vitro* (Supplementary Fig. S6B). Treatment with IFNγ also induced CXCL10 expression by the tumor cells (Supplementary Fig. S6A).

The immunogenicity of chemotherapeutics is usually related to the induction of immunogenic cell death (ICD), which plays a crucial role in the cross-presentation of tumor antigens by DCs to tumor-specific $CD8^+$ T cells. Bona fide ICD inducers such as anthracyclines induce ICD markers, including cell surface exposure of calreticulin (14). Although cisplatin is not regarded as bona fide ICD inducer (14), our *in vitro* studies revealed that hRT, cisplatin, or combination treatment with both induced the exposure of calreticulin, which was higher on day 6 than on day 4 or 2 after start of the treatment (Fig. 3F).

Together, these experiments demonstrated that cisplatin-based combination therapy induced CXCL10 in the nonirradiated secondary tumor, that the tumor cells can be a main source of this chemoattractant and that the CXCL10 expression by the tumor cells is not only induced by IFNγ (which *in vivo* is mainly secreted by lymphocytes) but also directly by cisplatin.

### The CXCL10/CXCR3 interaction is essential for the abscopal effect and the recruitment of $CD8^+$ T cells to the nonirradiated tumor upon triple therapy including cisplatin

To elucidate whether cisplatin- or cisplatin/anti–PD-1–induced CXCL10 is crucial for the recruitment of $CD8^+$ T cells to the nonirradiated tumor and therefore for the abscopal effect, we repeated the triple treatment with additional injections of the mAb CXCR3-173, which in C57BL/6 mice specifically blocks the interaction between CXCL10 and its receptor CXCR3 on T cells. This specificity arises because the CXCR3-173 mAb inhibits receptor binding of CXCL10 and CXCL11, but not CXCL9 (34), and because C57BL/6 mice do not express functional CXCL11 (35). In the B16-CD133 model, triple treatment in the presence of this mAb worsened the response of both the irradiated and the non-irradiated tumor to about the same extent as $CD8^+$ T-cell depletion did (Fig. 4A, Supplementary Fig. S7). Of note, the response of the nonirradiated metastasis was almost completely abrogated. In the MC38 model, CXCR3/CXCL10 blockade also led to a diminished response of the irradiated tumor, and the antitumor response of the nonirradiated secondary tumor completely depended on the CXCR3/CXCL10 interaction (Fig. 4B), very similar to the B16-CD133 model. The responses of both the large primary and the smaller secondary tumor were almost completely dependent on the CXCR3/CXCL10 interaction in tumor-bearing mice treated with cisplatin + anti–PD-1.

The proportion of $CXCR3^+$ $CD8^+$ T cells was particularly high in the secondary tumor, and this was almost invariably the case for the different treatment groups (Fig. 4C). However, when the CXCR3/CXCL10 interaction was blocked, total $CD8^+$ T cells and tumor-specific $CD8^+$ T cells were strongly reduced both in the irradiated and in the nonirradiated tumor, as shown in Fig. 4D for triple-treated mice. In contrast, the frequency of tumor-specific $CD8^+$ T cells in blood and secondary lymphatic organs remained similar (Fig. 4E).

These results demonstrate that the CXCR3/CXCL10 axis is crucial for infiltration of the nonirradiated tumor by $CD8^+$ T cells, including those induced by hRT + anti–PD-1 during the abscopal response.

### Direct cisplatin-mediated cytostatic and cytotoxic effects

Besides the induction of antitumor $CD8^+$ cytotoxic T cells and T-cell–attracting chemokines, cisplatin could aid abscopal effects through direct cytotoxic or cytostatic effects. As shown in Fig. 5A–D, testing a range of cisplatin concentrations *in vitro*, we found a dose-dependent reduction in the viability and numbers of tumor cells and in the proliferation marker Ki-67, and an increase in tumor cell death. These cisplatin doses correspond to serum concentrations found in cisplatin-treated patients with cancer (36). A reduction in $Ki\text{-}67^+$ tumor cells and an increase in apoptotic tumor cells were also found 48 hours after administering cisplatin (5 mg/kg) to mice bearing a B16-CD133 melanoma tumor with a size similar to that of the secondary tumor in the two-tumor model (Fig. 5E). These data demonstrated direct cytostatic and cytotoxic effects of cisplatin *in vivo*, which is in accordance with the tumor growth data in Fig. 1B (right), Supplementary Fig. S1C and S1D, and Fig. 1G. Such direct cytoreductive effects of cisplatin may also contribute to the radiotherapy-induced abscopal effect, by enhancing the effector-to-target ratio in the nonirradiated tumor (see also Supplementary Fig. S4).

### Transient radiotherapy-induced lymphopenia does not preclude effective local and abscopal tumor control

Radiation-induced lymphopenia could be an obstacle to effective combination radio-immunotherapies (37). Lymphopenia may also be induced by chemotherapy. We therefore examined whole-blood counts following the different treatment regimens. Interestingly, the single dose of cisplatin that was used throughout this study did not induce lymphopenia. When cisplatin was combined with anti–PD-1, the blood lymphocyte counts were even slightly increased (Fig. 6A and B). In treatment groups involving radiation (radiotherapy + anti–PD-1, cisplatin + radiotherapy, radiotherapy + cisplatin + anti–PD-1), a pronounced but only transient lymphopenia was observed (Fig. 6A and B). In contrast, neutrophils and monocytes were not decreased (Fig. 6C and D). Taken together, this experiment demonstrated that strong but transient

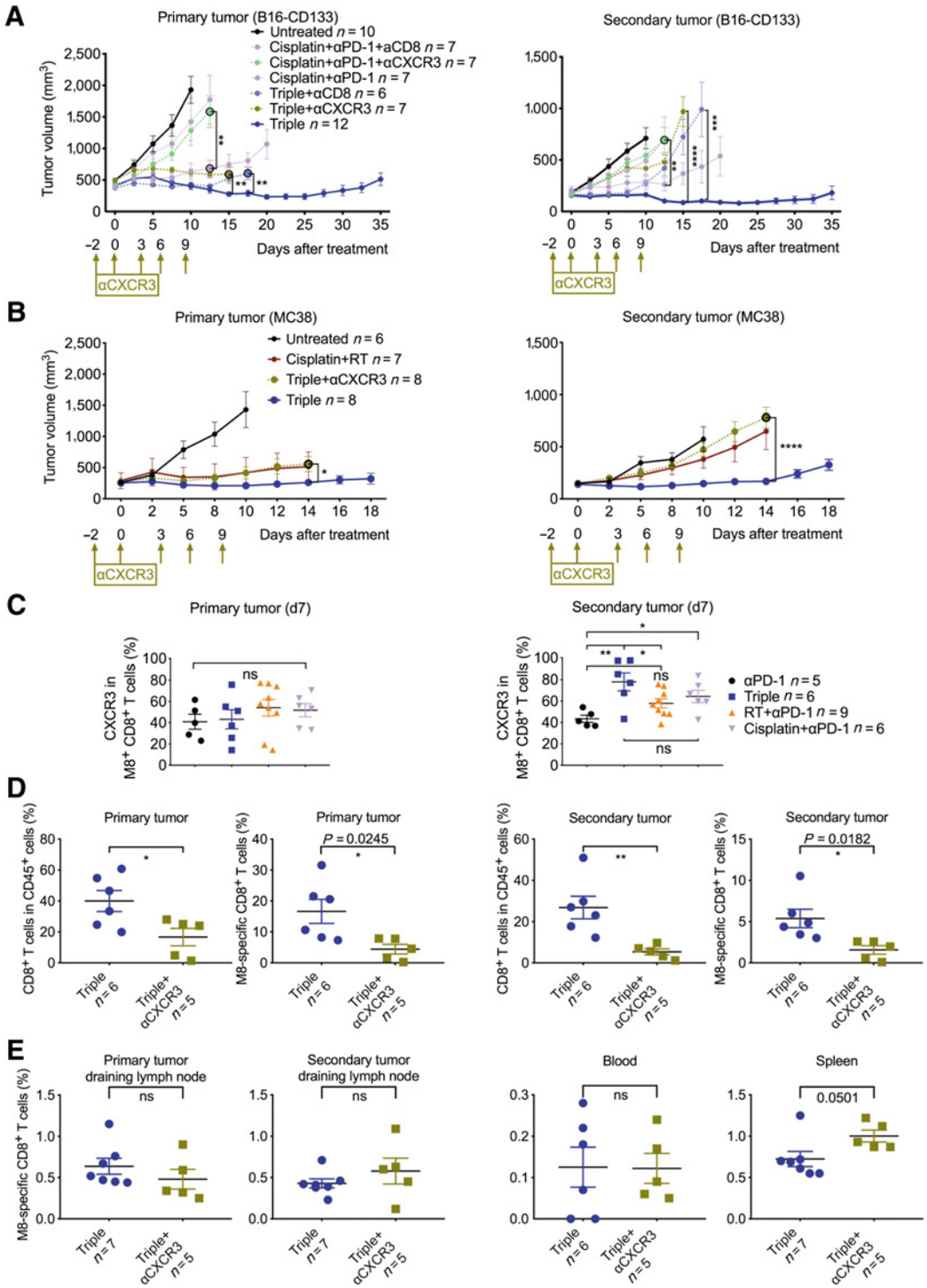


**Figure 4.**

CXCR3/CXCL10–mediated T-cell recruitment to nonirradiated tumor nodules is crucial for radiation-induced abscopal effects facilitated by cisplatin. **A,** Growth of irradiated primary (left) and nonirradiated secondary (right) B16-CD133 tumors (asterisks indicate *P* values for the comparison of certain groups as indicated in the figure). **B,** Growth of irradiated primary (left) and nonirradiated secondary (right) MC38 tumors (asterisks indicate *P* values for the comparison of certain groups as indicated in the figure). **C,** CXCR3-positive M8 tetramer-positive tumor-specific $CD8^+$ T cells on day 7 in the primary and secondary tumor for different treatment groups ($n = 5$–9 mice/group). **D,** Proportion of $CD8^+$ T cells and M8 tetramer-positive $CD8^+$ T cells in the $CD45^+$ subpopulation of tumor single-cell suspensions of the primary and secondary tumor on day 7 of triple treatment ± blockade of the CXCR3/CXCL10 interaction. **E,** M8 tetramer-positive tumor-specific $CD8^+$ T cells in the lymph nodes draining the primary and secondary tumor and in blood and spleen ($n = 5$–7 mice/group). All data are presented as mean ± SEM. ns, not significant; *, $P < 0.05$; **, $P < 0.01$; ***, $P < 0.001$; ****, $P < 0.0001$.

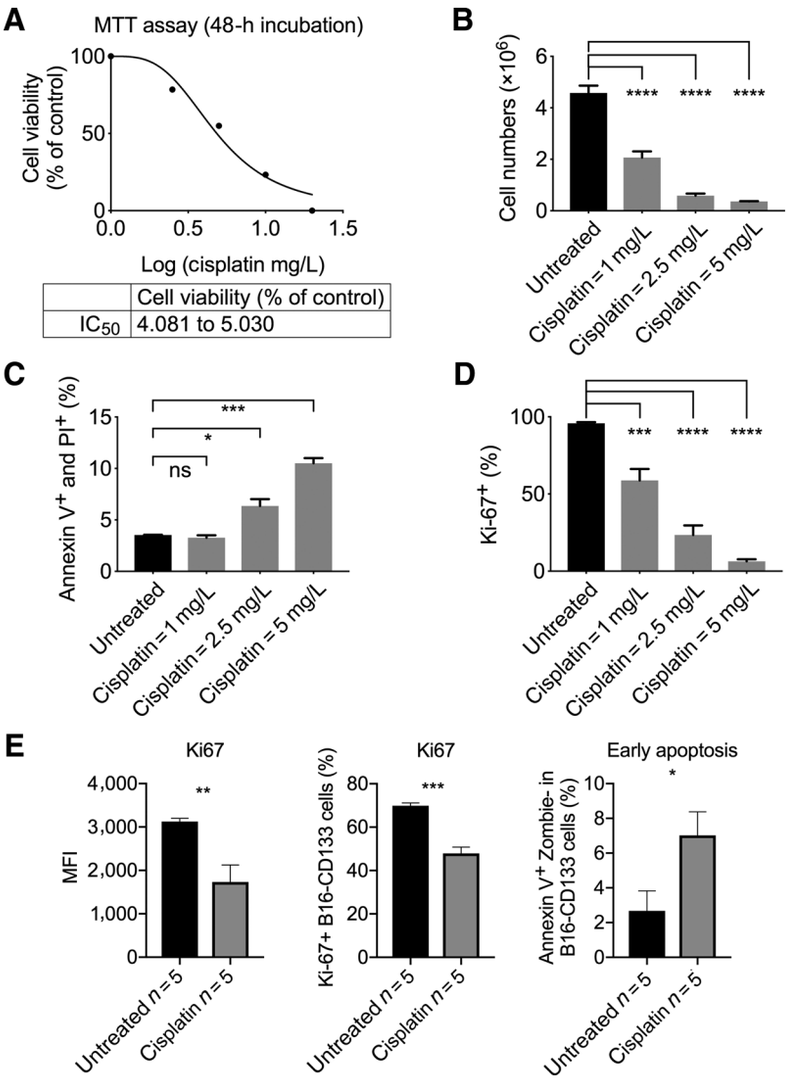


| | Cell viability (% of control) |
|---|---|
| $IC_{50}$ | 4.081 to 5.030 |

**Figure 5.**

Direct effects of cisplatin on the viability and proliferation of tumor cells *in vitro* and *ex vivo*. **A,** MTT assay for B16-CD133 cells treated with five different cisplatin concentrations (1, 2.5, 5, 10, 20 mg/L; $n = 10$ wells/concentration). **B,** Numbers of B16-CD133 cells after 48 hours of incubation with three different concentrations of cisplatin, counted microscopically after staining with Trypan blue (triplicates). **C,** Percentage of late apoptotic B16-CD133 cells after 48 hours of incubation with three different concentrations of cisplatin (triplicates). **D,** Ki-67–positive B16-CD133 cells after 48 hours of incubation with three different concentrations of cisplatin (triplicates). **E,** Percentage of Ki-67–positive and early apoptotic $CD133^+$ tumor cells and Ki-67 median fluorescence intensity (MFI) measured by flow cytometry in tumor cell suspensions directly *ex vivo* ($n = 5$ mice). All data are presented as mean with SEM. ns, not significant; *, $P < 0.05$; **, $P < 0.01$; ***, $P < 0.001$; ****, $P < 0.0001$.

lymphopenia does not preclude the strong radiotherapy-mediated abscopal effects as shown above.

## Discussion

Attempts to enhance ICB efficacy by radiotherapy in metastatic tumor patients and to induce abscopal effects have been based on irradiating one or a few tumor nodules. However, initial prospective clinical trials have only shown modest success of radiotherapy/ICB combinations in metastatic patients (6–11), and therefore, this approach has recently even been questioned by some authors (12, 13). Optimization or improvements are clearly needed.

Preclinical mechanistic investigations on how to achieve radiotherapy-induced abscopal effects have so far focused on how to optimally induce tumor-specific $CD8^+$ cytotoxic T cells by the irradiation (2, 28, 38). However, another crucial prerequisite for achieving an abscopal effect is that the induced T cells sufficiently infiltrate nonirradiated tumor nodules. Sufficient T-cell infiltration is generally regarded as one of the major obstacles in current cancer immunotherapy (39–43).

Furthermore, it is likely that additional drugs with direct cytoreductive effects facilitate radiotherapy-induced abscopal effects because they could enhance the ratio of tumor-specific T cells to tumor cells in the nonirradiated tumor nodules. Indeed, several recent articles have reported better anti–PD-1 responses in patients with lower tumor burden (44, 45). Cytotoxic effects should ideally be conferred by drugs that induce ICD. Some chemotherapeutic agents (mainly anthracyclines) are considered to be immunogenic and induce ICD mediators including T-cell–attracting chemokines (14, 19). Induction of T-cell–attracting chemokines has also been shown for radiotherapy (46, 47). However, cisplatin, the standard chemotherapeutic agent in radiation oncology, which is also widely used elsewhere in oncology for the treatment of numerous cancer entities including bladder, head-and-neck, lung, ovarian, and testicular cancers, is not regarded as a typical ICD inducer (14). Nevertheless, beneficial effects of platinum-based chemoradiation in combination with adjuvant anti–PD-L1 have already been reported for patients with locally advanced lung cancer without overt metastases (48). Additive effects were also reported for local growth suppression of single irradiated

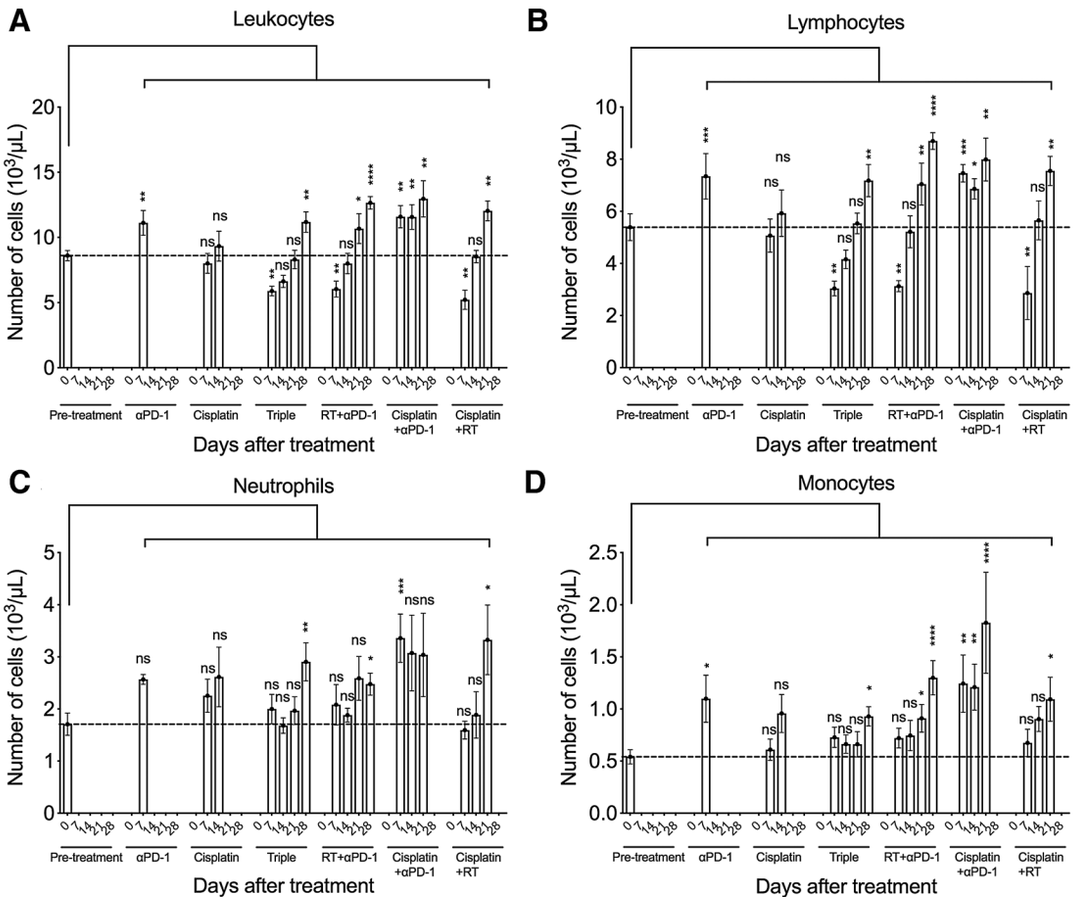


**Figure 6.**

Transient radiotherapy (RT)-induced lymphopenia. Number of leukocytes (**A**), lymphocytes (**B**), neutrophils (**C**), and monocytes (**D**) per μL peripheral blood at day 0, 7, 14, 21, and 28 of therapy for the treatments indicated (baseline measurement: 12 mice; triple therapy: eight mice; anti–PD-1 alone: seven mice; cisplatin alone: eight mice; radiotherapy + anti–PD-1: 11 mice; cisplatin + anti–PD-1: nine mice; cisplatin + radiotherapy: five mice. One-way ANOVA was used to compare the values between baseline and other time points. All data are presented as mean ± SEM. ns, not significant; *, $P < 0.05$; **, $P < 0.01$; ***, $P < 0.001$; ****, $P < 0.0001$.

tumors in mice after chemoradioimmunotherapy with anti–PD-L1 and gemcitabine (49) which is also not regarded as a typical ICD inducer (14).

Recently, Kroon and colleagues (25) investigated the effect of adding cisplatin to hRT + anti–PD-1 + anti-CD137 in a two-tumor model. In that model, cisplatin improved the response of the smaller nonirradiated tumor; hRT was necessary to sufficiently suppress the larger primary tumor. However, the model was not based on an radiotherapy-induced abscopal effect because the nonirradiated tumor was similarly controlled following hRT + anti–PD-1 + anti-CD137 versus anti–PD-1 + anti-CD137 and following hRT + anti–PD-1 + anti-CD137 + cisplatin versus anti–PD-1 + anti-CD137 + cisplatin.

In contrast, in the tumor models used by us, the hRT/anti–PD-1 double combination already caused a slight (MC38, C51) or moderate (B16-CD133) abscopal effect, but only in the form of a growth retardation of the nonirradiated tumor. Of note, this radiotherapy-induced abscopal effect was strongly enhanced by a single dose of cisplatin; in half of the B16-CD133 tumor-bearing mice, the triple treatment with hRT + anti–PD-1 + cisplatin cured the nonirradiated tumor, and in the remaining mice, temporary regression of the nonirradiated tumor was observed. In the C51 model, five of six mice were cured at the abscopal site, whereas this was only the case for one of seven mice treated with cisplatin + anti–PD-1 and for no mouse treated with hRT + anti–PD-1. Additional administration of other ICBs, such as anti-CD137 (25, 50), was not necessary. In all three tumor models, the triple combination was much more effective than either hRT + anti–PD-1 or cisplatin + anti–PD-1. However, in the radioresistant tumor models (B16-CD133 and MC38), the response of the primary tumor was not complete under the conditions used, in part perhaps because of the very rapid growth kinetics of the large tumors. In the current study, we used nonablative hRT, which has been shown to effectively induce abscopal effects in mice (27, 28, 31). Future work will show whether other hRT doses and fractionation schemes may result in better responses of large tumors in radioresistant tumor models. It will also be of interest to find out whether an abscopal response against established metastases would also occur at the usual normal-

fractionated clinical radiotherapy schedules or at stereotactic schedules that are mostly of higher dose per fraction and total dose.

We demonstrate that the strongly enhanced abscopal effect depended on $CD8^+$ T cells and that the CXCR3/CXCL10 interaction (51) is crucial for it and also for the infiltration of the nonirradiated abscopal tumor by $CD8^+$ T cells (Supplementary Fig. S8). CXCL10 can be induced by IFNγ (32), which is mainly secreted by tumor-infiltrating immune cells. However, the tumor cell–intrinsic CXCL10 expression directly induced by cisplatin, which we observed, has the great advantage that a prior successful T-cell infiltration of the nonirradiated abscopal tumors may be less important.

Nevertheless, we found that the cisplatin/anti–PD-1 double combination induced some tumor-specific $CD8^+$ T cells. Moreover, primary and secondary tumor responses were reduced when $CD8^+$ T cells were depleted in cisplatin/anti–PD-1-treated mice. The cisplatin/anti–PD-1-mediated induction of tumor-specific $CD8^+$ T cells may be facilitated by the cisplatin-induced cell surface exposure of calreticulin on tumor cells. In addition, our *in vitro* experiments indicate that a direct cytotoxic/cytostatic effect of cisplatin also contributes to the enhanced abscopal effect. Direct cytotoxic/cytostatic effects of cisplatin likely facilitate attacks by radiochemoimmunotherapy-induced $CD8^+$ T cells in nonirradiated tumor nodules. Our findings of tumor-specific $CD8^+$ T-cell induction in the nonirradiated tumor upon treatment with cisplatin + anti–PD-1 and the direct, cisplatin-induced expression of CXCL10 in the tumor cells demonstrate that cisplatin is immunogenic on its own. It will be of interest to find out whether radiosensitization by cisplatin at the site of the irradiated tumor contributes to the immunogenicity of cisplatin.

Finally, our data show that the pronounced, transient hRT-induced lymphopenia did not prevent effective local and abscopal antitumor T-cell responses. The single dose of cisplatin did not induce lymphopenia.

This is the first report showing that chemotherapy can enhance radiotherapy-induced abscopal effects in conjunction with ICB. Our data could be the basis for clinical trials in metastatic tumor patients. Such trials could clarify whether radiochemoimmunotherapy based on the irradiation of one or more tumor nodules, together with systemic cisplatin, enhances radiotherapy-induced abscopal effects and increases the efficacy of ICB and of combined chemotherapy and ICB. However, currently, metastatic tumor patients are not usually treated with chemoradiotherapy. Therefore, trials of concurrent radiochemoimmunotherapy would require a significant paradigm shift in the management of metastatic cancers. Moreover, we here used only one dose of cisplatin. Future studies will show how clinically more typical schedules, such as 3-weekly cisplatin administration, influence radiotherapy-induced abscopal effects in conjunction with ICB.

## Disclosure of Potential Conflicts of Interest

No potential conflicts of interest were disclosed.

## Authors' Contributions

**Conception and design:** R. Luo, G. Niedermann
**Development of methodology:** R. Luo, E. Firat
**Acquisition of data (provided animals, acquired and managed patients, provided facilities, etc.):** R. Luo, E. Firat, S. Gaedicke, E. Guffart
**Analysis and interpretation of data (e.g., statistical analysis, biostatistics, computational analysis):** R. Luo, E. Firat, T. Watanabe, G. Niedermann
**Writing, review, and/or revision of the manuscript:** R. Luo, E. Firat, S. Gaedicke, E. Guffart, G. Niedermann
**Administrative, technical, or material support (i.e., reporting or organizing data, constructing databases):** R. Luo, E. Guffart, G. Niedermann
**Study supervision:** G. Niedermann

## Acknowledgments

The authors gratefully acknowledge the financial support to Ren Luo from the China Scholarship Council. We thank the members of the Pahl lab (University of Freiburg) for providing the hematology analyzer.

The costs of publication of this article were defrayed in part by the payment of page charges. This article must therefore be hereby marked *advertisement* in accordance with 18 U.S.C. Section 1734 solely to indicate this fact.

Received April 24, 2019; revised August 1, 2019; accepted August 29, 2019; published first September 10, 2019.

## References

1. Wei SC, Duffy CR, Allison JP. Fundamental mechanisms of immune checkpoint blockade therapy. Cancer Discov 2018;8:1069–86.
2. Weichselbaum RR, Liang H, Deng L, Fu YX. Radiotherapy and immunotherapy: a beneficial liaison? Nat Rev Clin Oncol 2017;14:365–79.
3. Rodriguez-Ruiz ME, Vanpouille-Box C, Melero I, Formenti SC, Demaria S. Immunological mechanisms responsible for radiation-induced abscopal effect. Trends Immunol 2018;39:644–55.
4. Lugade AA, Moran JP, Gerber SA, Rose RC, Frelinger JG, Lord EM. Local radiation therapy of B16 melanoma tumors increases the generation of tumor antigen-specific effector cells that traffic to the tumor. J Immunol 2005;174:7516–23.
5. Rodriguez-Ruiz ME, Rodriguez I, Leaman O, Lopez-Campos F, Montero A, Conde AJ, et al. Immune mechanisms mediating abscopal effects in radioimmunotherapy. Pharmacol Ther 2019;196:195–203.
6. Kwon ED, Drake CG, Scher HI, Fizazi K, Bossi A, van den Eertwegh AJ, et al. Ipilimumab versus placebo after radiotherapy in patients with metastatic castration-resistant prostate cancer that had progressed after docetaxel chemotherapy (CA184–043): a multicentre, randomised, double-blind, phase 3 trial. Lancet Oncol 2014;15:700–12.
7. Twyman-Saint Victor C, Rech AJ, Maity A, Rengan R, Pauken KE, Stelekati E, et al. Radiation and dual checkpoint blockade activate non-redundant immune mechanisms in cancer. Nature 2015;520:373–7.
8. Hiniker SM, Reddy SA, Maecker HT, Subrahmanyam PB, Rosenberg-Hasson Y, Swetter SM, et al. A prospective clinical trial combining radiation therapy with systemic immunotherapy in metastatic melanoma. Int J Radiat Oncol Biol Phys 2016;96:578–88.
9. Tang C, Welsh JW, de Groot P, Massarelli E, Chang JY, Hess KR, et al. Ipilimumab with stereotactic ablative radiation therapy: Phase I results and immunologic correlates from peripheral T cells. Clin Cancer Res 2017;23:1388–96.
10. Luke JJ, Lemons JM, Karrison TG, Pitroda SP, Melotek JM, Zha Y, et al. Safety and clinical activity of pembrolizumab and multisite stereotactic body radiotherapy in patients with advanced solid tumors. J Clin Oncol 2018;36:1611–8.
11. Formenti SC, Rudqvist NP, Golden E, Cooper B, Wennerberg E, Lhuillier C, et al. Radiotherapy induces responses of lung cancer to CTLA-4 blockade. Nat Med 2018;24:1845–51.
12. Weichselbaum RR. The 46th David A. Karnofsky Memorial Award Lecture: oligometastasis-from conception to treatment. J Clin Oncol 2018;36:3240–50.

13. Brooks ED, Chang JY. Time to abandon single-site irradiation for inducing abscopal effects. Nat Rev Clin Oncol 2019;16:123–35.
14. Galluzzi L, Buque A, Kepp O, Zitvogel L, Kroemer G. Immunogenic cell death in cancer and infectious disease. Nat Rev Immunol 2017;17: 97–111.
15. Gandhi L, Rodriguez-Abreu D, Gadgeel S, Esteban E, Felip E, De Angelis F, et al. Pembrolizumab plus chemotherapy in metastatic non-small-cell lung cancer. N Engl J Med 2018;378:2078–92.
16. Schmid P, Adams S, Rugo HS, Schneeweiss A, Barrios CH, Iwata H, et al. Atezolizumab and nab-paclitaxel in advanced triple-negative breast cancer. N Engl J Med 2018;379:2108–21.
17. Tesniere A, Schlemmer F, Boige V, Kepp O, Martins I, Ghiringhelli F, et al. Immunogenic death of colon cancer cells treated with oxaliplatin. Oncogene 2010;29:482–91.
18. Lesterhuis WJ, Punt CJ, Hato SV, Eleveld-Trancikova D, Jansen BJ, Nierkens S, et al. Platinum-based drugs disrupt STAT6-mediated suppression of immune responses against cancer in humans and mice. J Clin Invest 2011; 121:3100–8.
19. Sistigu A, Yamazaki T, Vacchelli E, Chaba K, Enot DP, Adam J, et al. Cancer cell-autonomous contribution of type I interferon signaling to the efficacy of chemotherapy. Nat Med 2014;20:1301–9.
20. Beyranvand Nejad E, van der Sluis TC, van Duikeren S, Yagita H, Janssen GM, van Veelen PA, et al. Tumor eradication by cisplatin is sustained by CD80/86-mediated costimulation of CD8+ T cells. Cancer Res 2016;76: 6017–29.
21. Nolan E, Savas P, Policheni AN, Darcy PK, Vaillant F, Mintoff CP, et al. Combined immune checkpoint blockade as a therapeutic strategy for BRCA1-mutated breast cancer. Sci Transl Med 2017;9: pii:eaal4922.
22. Tran L, Allen CT, Xiao R, Moore E, Davis R, Park SJ, et al. Cisplatin alters antitumor immunity and synergizes with PD-1/PD-L1 inhibition in head and neck squamous cell carcinoma. Cancer Immunol Res 2017;5: 1141–51.
23. Kelland L. The resurgence of platinum-based cancer chemotherapy. Nat Rev Cancer 2007;7:573–84.
24. Szturz P, Wouters K, Kiyota N, Tahara M, Prabhash K, Noronha V, et al. Low-Dose vs. High-Dose cisplatin: lessons learned from 59 chemoradiotherapy trials in head and neck cancer. Front Oncol 2019; 9:86.
25. Kroon P, Frijlink E, Iglesias-Guimarais V, Volkov A, Van Buuren MM, Schumacher TN, et al. Radiotherapy and cisplatin increase immunotherapy efficacy by enabling local and systemic intratumoral T-cell activity. Cancer Immunol Res 2019;7:670–82.
26. Hettich M, Lahoti J, Prasad S, Niedermann G. Checkpoint antibodies but not T cell-recruiting diabodies effectively synergize with TIL-Inducing gamma-Irradiation. Cancer Res 2016;76:4673–83.
27. Rodriguez-Ruiz ME, Rodriguez I, Garasa S, Barbes B, Solorzano JL, Perez-Gracia JL, et al. Abscopal effects of radiotherapy are enhanced by combined immunostimulatory mAbs and are dependent on CD8 T cells and cross-priming. Cancer Res 2016;76:5994–6005.
28. Vanpouille-Box C, Alard A, Aryankalayil MJ, Sarfraz Y, Diamond JM, Schneider RJ, et al. DNA exonuclease Trex1 regulates radiotherapy-induced tumour immunogenicity. Nat Commun 2017;8:15618.
29. Jing H, Hettich M, Gaedicke S, Firat E, Bartholomä M, Niedermann G. Combination treatment with hypofractionated radiotherapy plus IL-2/anti-IL-2 complexes and its theranostic evaluation. J ImmunoTherapy Cancer 2019;7:55.
30. Spranger S, Dai D, Horton B, Gajewski TF. Tumor-residing Batf3 dendritic cells are required for effector T cell trafficking and adoptive T cell therapy. Cancer Cell 2017;31:711–23.
31. Zhang X, Niedermann G. Abscopal effects with hypofractionated schedules extending into the effector phase of the tumor-specific T-Cell response. Int J Radiat Oncol Biol Phys 2018;101:63–73.
32. Chow MT, Luster AD. Chemokines in cancer. Cancer Immunol Res 2014;2: 1125–31.
33. Hong M, Puaux AL, Huang C, Loumagne L, Tow C, Mackay C, et al. Chemotherapy induces intratumoral expression of chemokines in cutaneous melanoma, favoring T-cell infiltration and tumor control. Cancer Res 2011;71:6997–7009.
34. Uppaluri R, Sheehan KC, Wang L, Bui JD, Brotman JJ, Lu B, et al. Prolongation of cardiac and islet allograft survival by a blocking hamster anti-mouse CXCR3 monoclonal antibody. Transplantation 2008;86:137–47.
35. Sierro F, Biben C, Martinez-Munoz L, Mellado M, Ransohoff RM, Li M, et al. Disrupted cardiac development but normal hematopoiesis in mice deficient in the second CXCL12/SDF-1 receptor, CXCR7. Proc Natl Acad Sci U S A 2007;104:14759–64.
36. Go RS, Adjei AA. Review of the comparative pharmacology and clinical activity of cisplatin and carboplatin. J Clin Oncol 1999;17:409–22.
37. Ko EC, Formenti SC. Radiotherapy and checkpoint inhibitors: a winning new combination? Ther Adv Med Oncol 2018;10:1758835918768240.
38. Ko EC, Benjamin KT, Formenti SC. Generating antitumor immunity by targeted radiation therapy: role of dose and fractionation. Adv Radiat Oncol 2018;3:486–93.
39. Tumeh PC, Harview CL, Yearley JH, Shintaku IP, Taylor EJ, Robert L, et al. PD-1 blockade induces responses by inhibiting adaptive immune resistance. Nature 2014;515:568–71.
40. Nagarsheth N, Wicha MS, Zou W. Chemokines in the cancer microenvironment and their relevance in cancer immunotherapy. Nat Rev Immunol 2017;17:559–72.
41. Spranger S, Gajewski TF. Impact of oncogenic pathways on evasion of antitumour immune responses. Nat Rev Cancer 2018;18:139–47.
42. Zhang J, Endres S, Kobold S. Enhancing tumor T cell infiltration to enable cancer immunotherapy. Immunotherapy 2019;11:201–13.
43. Bonaventura P, Shekarian T, Alcazer V, Valladeau-Guilemond J, Valsesia-Wittmann S, Amigorena S, et al. Cold tumors: A therapeutic challenge for immunotherapy. Front Immunol 2019;10:168.
44. Huang AC, Postow MA, Orlowski RJ, Mick R, Bengsch B, Manne S, et al. T-cell invigoration to tumour burden ratio associated with anti-PD-1 response. Nature 2017;545:60–5.
45. Warner AB, Postow MA. Bigger is not always better: tumor size and prognosis in advanced melanoma. Clin Cancer Res 2018;24:4915–7.
46. Matsumura S, Wang B, Kawashima N, Braunstein S, Badura M, Cameron TO, et al. Radiation-induced CXCL16 release by breast cancer cells attracts effector T cells. J Immunol 2008;181:3099–107.
47. Meng Y, Efimova EV, Hamzeh KW, Darga TE, Mauceri HJ, Fu YX, et al. Radiation-inducible immunotherapy for cancer: senescent tumor cells as a cancer vaccine. Mol Ther 2012;20:1046–55.
48. Antonia SJ, Villegas A, Daniel D, Vicente D, Murakami S, Hui R, et al. Durvalumab after chemoradiotherapy in stage III non-small-cell lung cancer. N Engl J Med 2017;377:1919–29.
49. Azad A, Yin Lim S, D'Costa Z, Jones K, Diana A, Sansom OJ, et al. PD-L1 blockade enhances response of pancreatic ductal adenocarcinoma to radiotherapy. EMBO Mol Med 2017;9:167–80.
50. Chester C, Sanmamed MF, Wang J, Melero I. Immunotherapy targeting 4–1BB: mechanistic rationale, clinical results, and future strategies. Blood 2018;131:49–57.
51. Mikucki ME, Fisher DT, Matsuzaki J, Skitzki JJ, Gaulin NB, Muhitch JB, et al. Non-redundant requirement for CXCR3 signalling during tumoricidal T-cell trafficking across tumour vascular checkpoints. Nat Commun 2015;6: 7458.